# FACTORIAL DESIGN APPLIED TO CORROSION OF SUPERDUPLEX STAINLESS STEEL

T.J. MESQUITA†, R.P. NOGUEIRA† and I.N. BASTOS‡

† *UMR5266 and 5631 INP Grenoble-CNRS-UJF, SIMAP and LEPMI, BP 75, 38402 St Martin d'Hères, France*
*Thiago-Jose.Mesquita@lepmi.grenoble-inp.fr*
‡ *Instituto Politécnico / Universidade do Estado do Rio de Janeiro, Nova Friburgo-RJ, 28630-050, Brazil*
*ivan.bastos@pq.cnpq.br*

***Abstract*— Steels employed in offshore oil and gas production are subject to a very corrosive environment. Especially the new oilfields located in pre-salt layers imply the contact of steels with high brine concentration, high temperature and presence of corrosive gas such as $CO_2$. Besides these facts, stainless steels have to present higher mechanical properties obtained from an optimized heat treatment. In order to take into account these factors and their synergisms, on the present paper, we have chosen a factorial experimental design to study the corrosion behavior of superduplex steel UNS S32750 by electrochemical tests. The results of open circuit potential, polarization curves and electrochemical impedance were analyzed with statistical methods considering a confidence level of 95%. The factors that significantly affect the corrosion potential are the carbon dioxide and heat treatment; the corrosion current is sensitive to carbon dioxide, and the resistance of polarization is strongly affected by the $CO_2$ content.**

***Keywords*— superduplex stainless steel, polarization, factorial design**

## I. INTRODUCTION

The use of design of experiments in corrosion field is relatively limited, albeit the inherent advantages such as the improvement of process yield, reduction of development time and also can reveal the key-parameters that impact the final performance of material properties. In this sense, we can cite the following works where corrosion was investigated by factorial design (Pariona and Muller, 1998; Meng *et al.*, 2007; Hajeeh, 2003).

The presence of $CO_2$ promotes the so-called sweet corrosion that attacks the facilities made of low alloy steels in oil and transportation plants. In these contexts, a solution for these industries is the use of inhibitors for carbon steels (Paolinelli *et al.*, 2008; Linter and Burstein, 1999; Carvalho *et al.*, 2005) or to choose corrosion resistance alloys (CRA) which are more expensive than carbon steels. The modern duplex, superduplex and hyperduplex stainless steels present high corrosion and mechanical resistances, but they are not immune to corrosion in high aggressive chloride conditions (Deng *et al.*, 2008; Bastos *et al.*, 2007). Indeed, for the superduplex, the interplay between microstructure and localization of anodic and cathodic process is a key-factor of the corrosion intensity (Tsai and Chen, 2007) mainly for localized corrosion (Bastos and Nogueira, 2008).

The choice of using duplex stainless steels instead of the wide spread 300-series for chemical and petrochemical applications occurs thanks to their higher mechanical properties and to less susceptibility to chloride stress corrosion cracking and pitting (Gunn, 2003). In addition, their prices are competitive for some offshore applications. However, the complex microstructure, chiefly formed of ferrite and austenite, allows diverse heat treatments in which phases precipitate by time-temperature transformations. These rich microstructure scenarios, the peculiarities of corrosion resistance and the ever increasing demand for this steel grade make them very attractive to be studied. Thus, in the present paper we have shown how carbon dioxide, brine concentration and temperature affect the corrosion of UNS S32750 steel with two microstructural conditions. After the previous study of localized corrosion for this material (Bastos *et al.*, 2007, Bastos and Nogueira, 2008), in this paper, we have focused on the uniform corrosion because this is the main corrosion form of carbon steel in oil and gas plants, and the S32750 is a candidate to substitute the ordinary steel and other stainless steels. The CRA exhibit good resistance to uniform corrosion in the majority of industrial environment and their weakness is mainly the localized corrosion. Indeed, vast quantity of published work is devoted to study the localized corrosion. However, the investigation of uniform corrosion is also necessary, chiefly in industrial conditions that are challenging even for CRA, as is the case of pre-salt oilfields. To account for this aggressiveness, new alloys have been developed and consequently the corrosion properties must be known. We have chosen the chloride content, temperature and carbon dioxide typical of those present in actual pre-salt oilfields. In the present work, we focus on the study of the effect of pre-salt environment in the general corrosion of UNS S32750 alloy.

## II. MATERIALS AND METHODS

### A. Materials

Samples of UNS S32750 stainless steel were heat treated at 800°C for ¼ hour and 2 hours so as to yield two distinct microstructures. For the sake of simplicity, we will call these microstructures as M¼ and M2. This procedure allows the formation of deleterious phases

such as sigma, which degrade the corrosion resistance, as discussed elsewhere (Bastos *et al.*, 2007).

The samples were attacked by Behara´s solution to reveal the microstructure and then they were observed by optical microscopy.

The solutions used for the electrochemical experiments were prepared with NaCl in order to produce two high chloride contents (70.000 and 140.000 ppm) because these concentrations can occur during the oil processing. The temperatures of 30 and 60°C were set before immersion of samples, as well as the saturation of solution with carbon dioxide gas in specific cases.

Prior to electrochemical measurements, the sample surfaces were gritted with emery paper up to # 600, washed with distilled water and dried with hot air. The performed corrosion tests consist of monitoring the free corrosion potential for one hour, followed by electrochemical impedance spectroscopy (10 mVpp, 5 m-60 kHz) at corrosion potential and subsequently a polarization curve swept at a scan rate of 1.0 mV/s from 200 mV below corrosion potential up to 1.0 Vsce. All potential refers to saturated calomel electrode (sce).

Finally, these tests enabled many corrosion parameters to be obtained, such as: - corrosion potential, impedance modulus, corrosion current density, and polarization resistance. The significances of data were tested with statistical method described in the next section. Besides the statistical approach, the usual discussion of electrochemical behavior is also presented.

### B. Factorial Method

We use a single replicate of 16 experiments to study the corrosion behavior of a superduplex stainless steel UNS S32750. The orthogonal $2^4$ design reveals the main effect as well as the synergism of them. The chosen factors are likely to occur in extra-deep offshore oil extraction: salinity (A), temperature (B), heat treatment exposure (C) and presence of $CO_2$ gas (D). The uncodified levels of factors are presented in Table 1. The single $2^4$ factorial experimental designs in the codified mode are depicted in Table 2. Each number in this table represents one experience. The factorial design allows the evaluation of main effects as well as their mutual interactions. Each experiment was performed in randomized way to reduce systematic errors. The conditions depicted in Table 1 occur in offshore oil and gas exploitation, mainly in locations named pre-salt. The Brazilian huge oil and gas reserves are located in geologic sites where similar conditions are present. As the number of factor is relatively high, it is convenient the use of statistics to evaluate the significance of factors.

Table 1 – Factors employed in the experiments.

| Level | **A** – Salinity (NaCl ppm) | **B** – Temp. (°C) | **C** – Heat treatment time at 800°C (s) | **D** – $CO_2$ |
|---|---|---|---|---|
| Low - | 70.000 | 30 | 900 | absent |
| High+ | 140.000 | 60 | 7200 | saturation |

Table 2 - Factorial experimental design codified factor for corrosion tests.

| Factor | Experiment 1 2 3 4 5 6 7 8 9 10 11 12 13 14 15 16 |
|---|---|
| A | - + - + - + - + - + - + - + - + |
| B | - - + + - - + + - - + + - - + + |
| C | - - - - + + + + - - - - + + + + |
| D | - - - - - - - - + + + + + + + + |

The statistical data treatment was accomplished through the software Minitab 15 that uses the analyses of variance to determine the significance of factors. As the number of factor is relatively high, 4, we apply the principle of sparsity of effects, that is, the system is dominated by the main factors and low-order interactions, *i.e.*, there is an expectation that the higher order effects must be of minor statistical importance. Consequently, the error can be evaluated by the higher order of interactions. A procedure to check this model consists of plotting the effects in a normal distribution. The negligible factors fall along a straight line, whilst the significant ones lay out of the line.

The statistical significance test evaluates the F-ratio (square of effects/square of residuals). If the calculated F is higher than a $F_o$ for a given significance level (usually 0.05) and a given degree of freedom, this effect is considered as statistically significant, otherwise, is unimportant. A reference about design of experiment was presented in Montgomery and Runger (1994).

## III. RESULTS AND DISCUSSION

Both M¼ and M2 microstructures are depicted in Fig. 1. The sample treated for a shorter time still preserve its duplex microstructure consisting of austenite and ferrite in roughly equal proportion, but the long time exposition promotes a strong changing in the microstructure. Indeed, the heat treatments performed during 2 hours show, besides a duplex structure, the grain boundary precipitation and also the sigma phase (σ) formation in the ferrite phase. A more detailed discussion about the phase transformation is found elsewhere (Bastos *et al*, 2007). Anyway, as the metallurgical condition changes, there is a modification of localized corrosion resistance. In addition, the specific metallurgical regions can work as anodic or cathodic sites as described by Tsai and Chen (2007) and this dissimilarity favors the local dissolution. However, in the present paper we addressed mainly the uniform behavior near the free corrosion potential because it is the situation more related to real application.

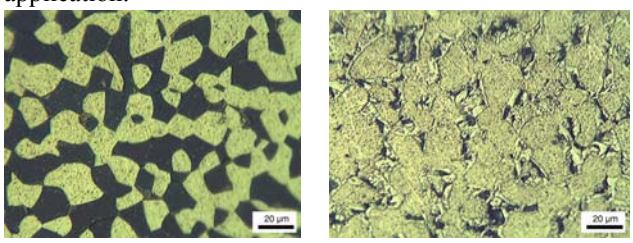


900 s at 800°C (M¼) 72000 s at 800°C (M2)

Figure 1 – Microstructures of heat treated UNS S32750.

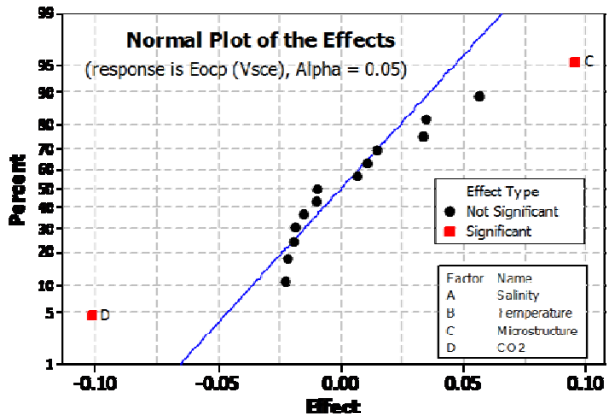


Figure 2 – Normal distribution of effects related to open circuit potential.

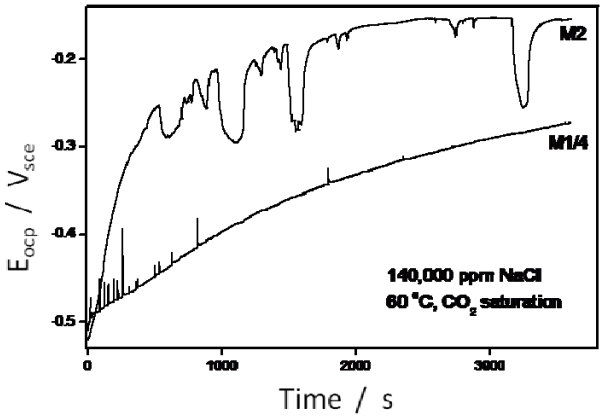


Figure 3 – Evolution of open circuit potential of M¼ and M2 at 60°C and $CO_2$ saturation.

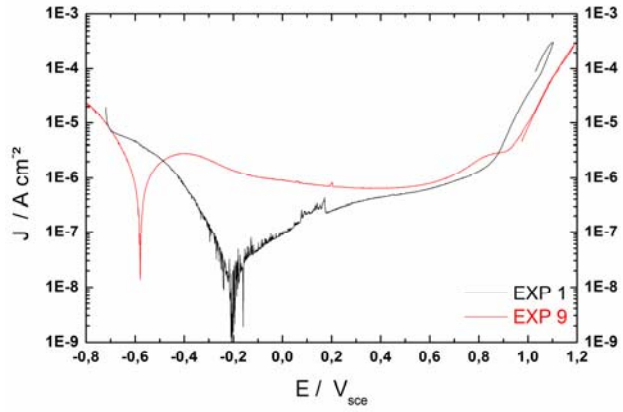


Figure 4 – Polarization curve of experiments 1 and 9.

The statistical distribution of effects related to the free corrosion potential obtained after a time delay of one hour is presented in Fig. 2. The data refer to a set of 15 results: 4 main effects (A, B, C, and D factors of Table 1), 6 two-factor interactions, 4 three-factor interactions and 1 four-interaction, and not the electrochemical potential itself. The statistically significant parameters are the microstructure (C) and carbon dioxide (D). More precisely, the negative values in the x-axis indicate that $CO_2$ tends to reduce Eocp, whilst long-lasting heat treatments at 800°C have an increasing effect on Eocp. Figure 3 (referred to experiments 12 and 16 of Table 2) illustrates the corrosion potential changes with immersion time. As the time goes on, the potential become nobler for both, but the M2 has a more erratic behavior, with broad fluctuations in negative sense, although its average value is superior to M¼. The saturation of $CO_2$ does not prevent the potential increase.

Stainless steel usually presents an increase of the open circuit potential with time as observed in Fig. 3, which is often related to the improvement of corrosion resistance as the result of passive film ageing. An additional effect related to the metal exposition at 800°C could be the solid-state diffusion of alloying elements that could induce the formation of a nobler passive layer. The diffusion during heat treatment occurs mainly in ferrite phase (Gunn, 2003). As a result, some precipitation occur giving rise to heterogeneous microstructures as depicted in Fig. 1. The several decays on the corrosion potential for the M2 microstructure could be associated to metastable localized corrosion, which means that each drop corresponds to the depassivation followed by the repassivation of the sample surface.

The obtained data confirm our hypothesis that all interactions of third and fourth orders are insignificant at a confidence interval of 0.05, at least for corrosion potential. Therefore, these interactions can be used to estimate the pooled evaluation of mean square error. Hereafter, the estimation of mean square error of others parameters will follow this methodology.

The normal distribution considered here is robust to model this data, since, in general, the design with a several independent factors tend to have a normal distribution as a consequence of central limit theorem.

Figure 4 shows the polarization curves of experiments 1 and 9. These curves were potentiodynamically performed and the corrosion current densities were obtained from these results using the traditional Tafel fitting. The surface analysis after the polarization curves do not reveal the presence of pits, as it is expected when the anodic current returns nearly in the same path with the reversion of applied potential as depicted in Fig. 4. The behavior of elevation of current intensity near 0.9 Vsce is related to the electrolyte oxidation instead of localized corrosion.

For the corrosion current density, the only relevant parameter, alone or combined with those of order superior than one, within the tested conditions is the $CO_2$, as shown in the Fig. 5. The carbon dioxide has a positive effect, which means that its presence augments the corrosion current. Indeed, the carbon dioxide is an important aggressive agent, mainly for carbon steels, and for the findings present here, it is also relevant for superduplex, at least for the considered confidence.

The saturation of $CO_2$ causes the acidification of the chloride medium, as illustrated in Fig. 6, due to the formation of carbonic acid by $CO_2$ hydration ($H_2O + CO_2 = H_2CO_3$). The bubbling of $CO_2$ can affect the anodic and cathodic process. The carbonic species acts as iron-ligand and accelerate the iron dissolution (Nešić, 2007). Although the effect of $CO_2$ in anodic branch of stainless steel in 0.5 M NaCl showed to be no measurable at

room temperature (Linter and Burstein, 1999), for the corrosion current density present here, related to super-duplex, the carbon dioxide modifies their values.

For sweet corrosion of iron, it is observed that the corrosion steadily decreases with pH in the region $4<pH<7$ (Nešić, 2007). A similar behavior is found for superduplex, as shown in Fig. 7. This effect is calculate as the difference between the average response in 8 high level of carbon dioxide experiments and the 8 low level ones, $D_{YES} = \sum_{9}^{16} icorr_i \Big/ 8$ and $D_{NO} = \sum_{1}^{8} icorr_i \Big/ 8$ respectively. From pH 4 to 8, all carbonic acid practically transforms into bicarbonate due to the first ionization of $H_2CO_3$ ($H_2CO_3 = H^+ + HCO_3^-$) under chemical equilibrium. The hydration curve of Fig. 6, performed at 60°C, indicates that the pH reaches the steady-state in a time inferior than approximately 200 s from the beginning of bubbling. Without carbon dioxide bubbling the pH is 7.2 and with addition, the pH is shifted to 4.0.

The behavior of the polarization resistance (Rp) reveals that carbon dioxide is very important, and negatively affects the Rp. In addition, the temperature also has a similar effect, but with less impact as evaluated by the distance between the given point and the line of normal distribution. A synergism with $CO_2$-temperature (second-order) occurs, and, as expected, the joint effect of these factors has a positive signal, although individually each factor has a negative effect. From the distance of straight line, its impact has approximately the same magnitude of that of temperature. Unfortunately, the correlation between Icorr and Rp was impossible to be obtained because in this case there is no degree of freedom in the unreplicated design. The relation between Rp and Icorr is complex because dependents on the actual mechanism of electrochemical reactions, but it can be roughly assumed to vary inversely as predict by Stern-Geary relationship. Summarizing, it is interesting to observe that $CO_2$ has positive effect on Icorr (Fig. 7), and negative one in Rp (Fig. 8).

The $CO_2$ bubbling in an aqueous solution reduces the pH, but for Linter and Burstein (1999) the pH itself is not the responsible for the corrosion behavior, since changing in pH does not completely emulates the comportment of carbon dioxide at least for carbon steel.

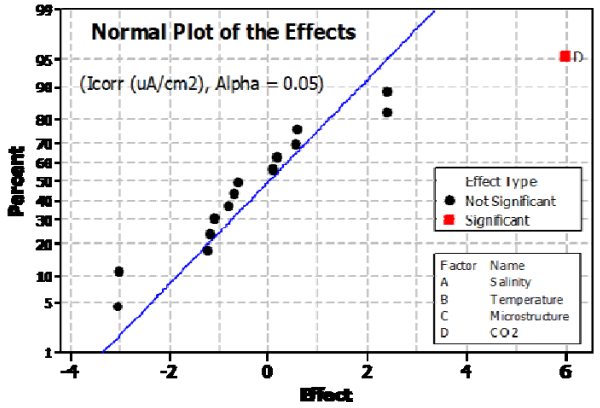


Figure 5 – Normal distribution of effects related to corrosion current density.

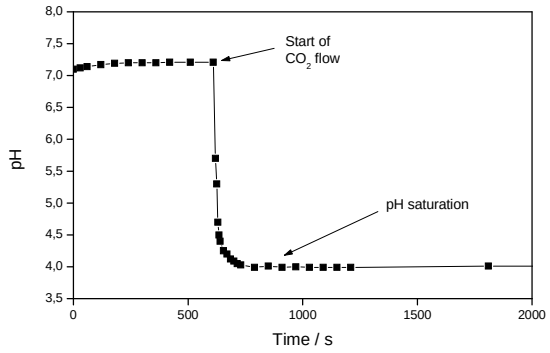


Figure 6 – Medium acidification by carbon dioxide.

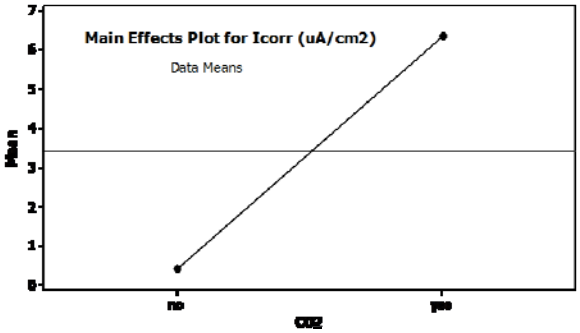


Figure 7 – Dependence of corrosion current on carbon dioxide presence.

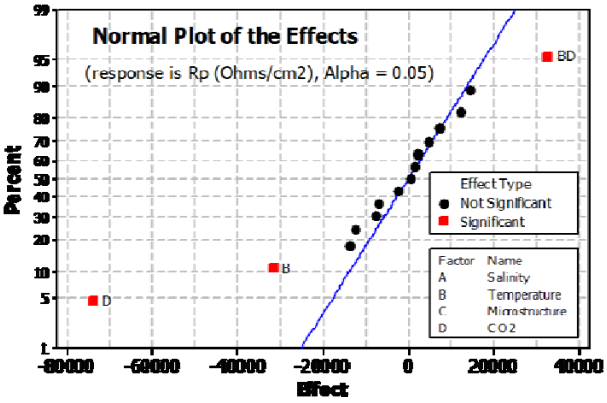


Figure 8 – Dependence of Rp on carbon dioxide and temperature.

Certain properties of the passive film can be characterized by electrochemical impedance spectroscopy – EIS. The complete impedance for Bode representation of experiments 1 and 9, for instance, is shown in Fig. 9. These tests were performed with salinity, temperature and exposure time at 800°C in low levels, and such way that the $CO_2$ effect can be observed. Moreover, from the angle phase results, there is a tendency of two time constant formation, but this behavior is found far beyond the frequency used in the factorial design discussion.

The EIS produces as result a complex diagram, thus to use the impedance results in design of experiment framework is necessary to choose one-dimensional parameter. In this way, we have chosen the impedance

modulus at low frequency, because it tends to Rp for null frequency. The normal distribution of parameters is shown in Fig. 10 and again the only relevant factor is the presence of carbon dioxide. In fact, the carbon dioxide played an important role in corrosion of the superduplex stainless steel, as shown in all electrochemical results.

## IV. CONCLUSIONS

An orthogonal design of experiment was carried out to investigate the corrosion of superduplex stainless steel UNS S32750 in two microstructural conditions. Thus a $2^4$ factorial design was implemented to analyze the electrochemical parameters of open circuit potential, corrosion current density, resistance polarization and electrochemical impedance. The physico-chemical conditions of electrolyte were the brine concentration of 70,000 and 140,000 ppm, temperature (30 and 60°C) and presence or not of carbon dioxide. The levels of brine concentrations were not relevant for the corrosion of both microstructures. The $CO_2$ bubbling had a strong statistical significance for all parameters within the studied conditions. Finally, the employed experimental conditions simulated a real application of this material such as it is found in ultra-deep oil exploitation.

## ACKNOWLEDGEMENT

This work was done under the INP-Grenoble-France and UERJ-Brazil accord. The authors would like to acknowledge the Brazilian agencies, FAPERJ and CNPq, for their financial supports.

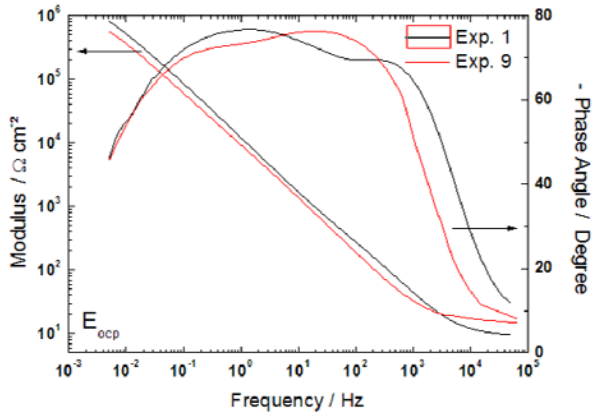


Figure 9 – Impedance diagram obtained at $E_{OCP}$.

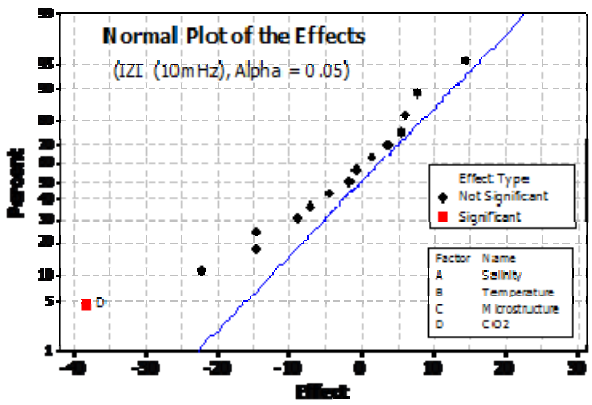


Figure 10 – Dependence of Rp on carbon dioxide and temperature.

## REFERENCES

Bastos, I.N. and R.P. Nogueira, "Electrochemical noise characterization of heat-treated superduplex stainless steel," *Mater. Chem. Phys*., **112**, 645-650 (2008).

Bastos, I.N., S.S.M. Tavares, F. Dalard and R.P. Nogueira, "Effect of microstructure on corrosion behavior of superduplex stainless steel at critical environment conditions," *Scripta Mater*., **57,** 913-916 (2007).

Carvalho, D.S., C.J.B. Joia and O.R. Mattos, "Corrosion rate of iron and iron–chromium alloys in $CO_2$ medium," *Corros. Sci*. **47**, 2974–2986 (2005).

Deng, B., Y. Jiang, J. Gong, C. Zhong, J. Gao and J. Li, "Critical pitting and repassivation temperatures for duplex stainless steel in chloride solutions," *Electrochim. Acta,* **53**, 5220–5225(2008).

Gunn, R.N. *Duplex stainless steels: microstructure, properties and applications*, Abington Publishing Ltd, Cambridge, England (2003).

Hajeeh, M., "Estimating corrosion: a statistical approach," *Materials and Design*, **24**, 509-518, (2003).

Linter, B.R. and G.T. Burstein, "Reactions of pipeline steels in carbon dioxide solutions," *Corros. Sci*., **41,** 117-139 (1999).

Montgomery, D.C. and G.C. Runger, *Applied Statistics and Probability for Engineers*, John Wiley & Sons, Inc., USA (1994).

Meng, H., X. Hu and A. Neville, "A systematic erosion–corrosion study of two stainless steels in marine conditions via experimental design," *Wear*, **263,** 355-362 (2007).

Nešić, S., "Key issues related to modelling of internal corrosion of oil and gas pipelines - A review", *Corros. Sci*. **49,** 4308–4338 (2007).

Paolinelli, L.D., T. Pérez and S.N. Simison, "The effect of pre-corrosion and steel microstructure on inhibitor performance in $CO_2$ corrosion," *Corros. Sci*., **50,** 2456–2464 (2008).

Pariona, M.M. and I.L. Muller, "Numerical simulation and factorial design of titanium crevice corrosion in sodium chloride solution," *Computers Chem*., **22**, 377-384 (1998).

Tsai, W-T and J-R Chen, "Galvanic corrosion between the constituent phases in duplex stainless steel," *Corros. Sci*., **49,** 3659-3668 (2007).

**Received: October 11, 2010**
**Accepted: December 14, 2010**
**Recommended by subject editor: Eduardo Dvorkin**